

RESEARCH ARTICLE

Open Access

Increased complexity of *Tmem16a*/Anoctamin 1 transcript alternative splicing

Kate E O'Driscoll, Rachel A Pipe and Fiona C Britton*

Abstract

Background: TMEM16A (Anoctamin 1; ANO1) is an eight transmembrane protein that functions as a calcium-activated chloride channel. *TMEM16A* in human exhibits alternatively spliced exons (6b, 13 and 15), which confer important roles in the regulation of channel function. Mouse *Tmem16a* is reported to consist of 25 exons that code for a 956 amino acid protein. In this study our aim was to provide details of mouse *Tmem16a* genomic structure and to investigate if *Tmem16a* transcript undergoes alternative splicing to generate channel diversity.

Results: We identified *Tmem16a* transcript variants consisting of alternative exons 6b, 10, 13, 14, 15 and 18. Our findings indicate that many of these exons are expressed in various combinations and that these splicing events are mostly conserved between mouse and human. In addition, we confirmed the expression of these exon variants in other mouse tissues. Additional splicing events were identified including a novel conserved exon 13b, tandem splice sites of exon 1 and 21 and two intron retention events.

Conclusion: Our results suggest that *Tmem16a* gene is significantly more complex than previously described. The complexity is especially evident in the region spanning exons 6 through 16 where a number of the alternative splicing events are thought to affect calcium sensitivity, voltage dependence and the kinetics of activation and deactivation of this calcium-activated chloride channel. The identification of multiple *Tmem16a* splice variants suggests that alternative splicing is an exquisite mechanism that operates to diversify TMEM16A channel function in both physiological and pathophysiological conditions.

Background

Alternative splicing of pre-mRNAs is a powerful regulatory mechanism that can increase mRNA transcript variety and effect functional diversification of proteins [1]. Within the cardiovascular system, alternative splicing affects cardiac function by regulating proteins involved in cellular excitation, including ion channels [2-8].

Calcium-activated chloride currents have been recorded in cardiac muscle cells from various species including mouse [9], and play an important role in the cardiac action potential [10-12]. In 2008, three independent groups identified *Tmem16a* as a strong candidate gene to encode (or at least a major component of) a calcium-activated chloride channel [13-15]. *Tmem16a* belongs to a family of ten mammalian paralogs (*Tmem16* (a-h, j-k)) that are highly conserved membrane spanning proteins. In recombinant expression systems, *Tmem16a* (or Anol1) and *Tmem16b*

(or Anol2) generate calcium-activated chloride currents [13-18] with similar biophysical and pharmacological properties to currents recorded from native tissues [19]. We and others have identified *Tmem16a* expression in mouse and human heart [20,21].

The human *TMEM16A* gene exhibits three alternatively spliced exons (6b, 13 and 15) as well as an alternative transcription start site [13]. Ferrera et al. reported that the biophysical properties of human TMEM16A are regulated by alternative splicing and *TMEM16A* splice variants form functional channels that display different properties [22]. The alternative exon 6b (encoding 22 amino acids) may play an important role in the regulation of the TMEM16A channel by calcium, since exclusion of this exon increases the calcium sensitivity of the channel ~ 4-fold [22]. Exon 13, encoding 4 amino acids, contributes significantly to TMEM16A channel kinetics, since exclusion of this exon significantly reduces the voltage dependence of activation [22]. A recent study showed that exon 15 (encoding 26 amino acids) exclusion results in significantly faster

* Correspondence: fbritton@medicine.nevada.edu
Department of Physiology and Cell Biology, 1664 North Virginia Street,
University of Nevada School of Medicine, Reno, Nevada 89557-0046, USA

activation and deactivation kinetics [23]. In addition, Mazzone et al, showed significant differences in expression of alternatively spliced *TMEM16A* exons in patients with diabetic gastroparesis when compared to non-diabetic controls [23]. Therefore, it appears that alternative splicing of human *TMEM16A* plays an important role in the regulation of calcium-activated chloride channel function.

The reported mouse *Tmem16a* gene [GenBank: NC_000073] is composed of 25 exons that code for a 956 amino acid protein [GenBank: NP_848757]. Unlike human, mouse *Tmem16a*, as annotated, does not contain alternative exons 6b, 13 or 15. We and others however, have reported that *Tmem16a* transcripts containing these alternative exons are expressed in mouse stomach, intestine [24] and vascular [25] smooth muscle tissues. It is likely that alternative splicing of *Tmem16a* transcript in mouse may lead to a number of different *TMEM16A* channel proteins with altered biophysical properties similar to human *TMEM16A* [22,23]. In this study our aim was to provide detailed information of the structure of the mouse *Tmem16a* gene and to investigate if *Tmem16a* transcript undergoes alternative splicing to generate channel diversity in mouse heart. This study demonstrates that the structure of *Tmem16a* gene is significantly more complex than previously indicated. The complexity is especially evident in the region containing exons 6 through 16. Determining the variation of *Tmem16a* transcript expression in heart is an important foundation for future studies of the physiological role of *Tmem16a* channels in heart.

Methods

RNA isolation and RT-PCR

Total RNA was isolated from mouse tissues using TRIzol reagent (Invitrogen, Carlsbad, CA). Human heart RNA was purchased from Agilent Technologies (Santa Clara, CA). First-strand cDNA was prepared from 1 µg of RNA using oligo(dT)₍₁₂₋₁₈₎ primer and Superscript II reverse transcriptase (Invitrogen). AmpliTaq Gold[®] PCR reagent (Applied Biosystems, Foster City, CA) was used to amplify each of the *Tmem16* paralogs and *Tmem16a* splice variants. PCR primers were designed using the mouse and human *Tmem16a* mRNA sequences [GenBank: NM_178642 and GenBank: NM_018043]. Details of the primer sets used are provided in additional file 1, Table S1 and Table S2). Glyceraldehyde-3-phosphate dehydrogenase (GAPDH) was used as a control for cDNA integrity. No template PCR reactions served as controls for primer contamination. PCRs were performed in a 2720 Thermal Cycler (Applied Biosystems). Amplification consisted of 95°C for 10 min, then 35 cycles of 95°C for 15 sec, T_a for 20 sec and 72°C for 30-60 sec, followed by a final step at 72°C for 7 min.

Splice variant identification, sequencing and bioinformatics

PCR products were resolved on 2-3% super fine agarose (Amresco, Solon, OH) gels along with a 100 bp molecular weight marker. *Tmem16a* amplification products were either purified (QIAquick Gel Extraction Kit, Qiagen, Valencia, CA) or TA cloned into the pcDNA3.1 vector (Invitrogen). All fragment sequencing was performed at the Nevada Genomics Center. Nucleotide and protein sequences were analyzed using Vector NTI version 11 software (Invitrogen) and BLASTN software at the National Center for Biotechnology Information (NCBI) database <http://www.ncbi.nlm.nih.gov/BLAST/>.

Transmembrane regions were predicted using the CBS TMHMM Server v 2.0 <http://www.cbs.dtu.dk/services/TMHMM/> and TMPred http://www.ch.embnet.org/software/TMPRED_form.html programs. The Tandem Splice Site DataBase (TassDB2) <http://gen100.imb-jena.de/TassDB2/> was used to confirm alternative tandem splice sites in mouse and human *Tmem16a*. The Scansite database http://scansite.mit.edu/motifscan_id.phtml was used to identify motifs in the *TMEM16A* alternative splice variants.

Results and Discussion

Tmem16a genomic structure is highly conserved in mouse and human

Genomic sequences for human [GenBank: NC_000011] and mouse [GenBank: NC_000073] *Tmem16a* were compared with their respective RNA sequence [GenBank: NM_018043 and NM_178642]. The reported mouse *Tmem16a* gene is composed of 25 exons, however, our analysis has revealed that mouse *Tmem16a* gene consists of at least 29 exons, ranging in size from 12 bp to 1621 bp. Table 1 provides details of mouse *Tmem16a* gene structure, including the number of exons, exon and intron size, 5' donor and 3' acceptor splice site sequences. The exon sizes of human *TMEM16A* are also provided for comparison purposes. The exon-intron junctions of *Tmem16a* comply with the consensus dinucleotide GT-AG rule. The number and size of each exon in mouse *Tmem16a* gene are highly conserved with human *TMEM16A*. There is some divergence between mouse and human *Tmem16a* genes at the 5' and 3' termini. For example, in mouse, exon 1 and exon 1b differ from human. The putative translational initiation codon of mouse and human *Tmem16a* are located in exon 1b and exon 1 respectively. The nucleotides adjacent to the initiator codons (mouse; GCCACCATGA and human; GCCACGATGA), constitute a favorable Kozak consensus initiation site [26]. Human *TMEM16A* has been reported to exhibit alternative splicing [13]. This study indicates that *Tmem16a* in mouse also exhibits multiple

Table 1 Genomic Organization of *Tmem16a*

Human				Mouse		
Exon number	Exon size (bp)	Exon number	Exon size (bp)	3' Acceptor and 5' Donor splice site sequences		Intron size (bp)
1	413	1	119		CAGGTG gt agga	~59,580
		1b	146	ttgc ag ACGCCA	GGCACG gt gagt	8,958
2	333	2	333	tcac ag TTGCTG	GAGGAT gt gagt	12,229
3	99	3	99	ctct ag ACCAAA	AAGAAG gt gagt	1,264
4	152	4	152	ccac ag GTGTAC	ACACCT gt gagt	1,340
5	55	5	55	ctgc ag ATTCGA	ACAATA gt gagt	3,649
6	52	6	52	ccct ag GTCTAT	GCATGG gt aagg	1,862
6b	66	6b	66	aaac ag GGCAAG	AATACG gt aaga	495
7	56	7	56	ttaa ag GTATCA	CACGAT gt aagt	3,274
8	42	8	42	tcac ag GGGGAC	AGGAAA gt aagt	6,143
9	65	9	65	cccc ag CTCCTG	GGTCAG gt aagt	1,290
10	135	10	135	gcat ag GAAATA	CCCCAG gt aggc	3,318
11	161	11	161	ttac ag TATGGA	TCTGGG gt aagt	11,845
12	83	12	83	ctac ag CTGCCA	GAGGAG gt gagt	2,181
13	12	13	12	ccgc ag GAAGCT	GTCAAG gt ttga	161
		13b	120	ttcc ag CACCTT	CAGAGG gt cagt	273
14	72	14	72	tctc ag GATCAT	AAAGAG gt acag	2,874
15	78	15	78	cctc ag AAGTGC	AAATTG gt tactt	972
16	75	16	75	ttgc ag ACCGAC	TTCATG gt aagt	3,034
17	202	17	202	ctgc ag ATCGCA	AGATTG gt gagt	167
18	112	18	112	cctc ag AGGTCC	AGGCCG gt agga	434
19	58	19	58	tccc ag GTTTGT	GAGGAG gt aata	1,892
20	101	20	101	ctac ag TGTGCC	CATCCC gt gagt	786
21	146	21	146	ctgc ag GAAGAT	AAATGA gt gagt	4,324
22	153	22	153	ctgc ag TCATTC	ACATCG gt aagt	6,207
23	53	23	53	ctct ag GCATCT	ATTAAT gt aagt	1,554
24	185	24	185	tggc ag GCCTTT	CTGCAG gt acta	2,635
25	106	25	106	ttgc ag GTATAA	TTCCAG gt atgt	2,435
26	1809	26	1621	ctgc ag AACCTG		

Intron size refers to the intron following the exon listed in each row.

alternative exons, which generates numerous isoforms through alternative splicing of the primary transcript. A close examination of the mouse *Tmem16a* genomic sequence revealed that similar sequences to these human exon variants (exons 6b, 13 and 15) could be identified (Table 1). Additionally, a number of novel splicing events were identified (Table 1) and the details of these transcript variants are outlined throughout this report.

Identification of *Tmem16a* splice variant expression in mouse heart

RT-PCR was initially used to identify the expression of *Tmem16* paralogs in mouse heart using primers specific for each of the *Tmem16* family members (Additional file 1, Table S1). In addition to *Tmem16a*, several other *Tmem16* transcripts were detected in mouse heart: *Tmem16c*, *d*, *e*, *f*, *h*, *j* and *k* (Figure 1A). The expression of *Tmem16b* and *Tmem16g* transcripts were not detected.

To determine if alternative exons, homologous to the exons 6b, 13 and 15 of human *TMEM16A* [13], are also expressed in mouse heart we performed RT-PCR analysis of *Tmem16a* (Figure 1B). Primer sets ± exon 6b, ± exon 13 and ± exon 15 amplify fragments that differ in size (± 66 bp, 12 bp and 78 bp, respectively) corresponding to the size of the alternative exon. The amplification of two fragments using ± exon 6b and ± exon 15 primers clearly indicates that *Tmem16a* variants that either include or exclude these alternative exons are expressed in mouse heart (Figure 1B). The presence or absence of the alternative 12 bp micro-exon 13 is difficult to resolve by gel electrophoresis, therefore additional primers were designed that either hybridize within each of the alternative exons to specifically amplify them or that span bordering exons to exclude them (Figure 1C and Additional file 1, Table S2). For example, *Tmem16a* transcripts lacking exon 15 (-exon 15) were selectively amplified using a primer that

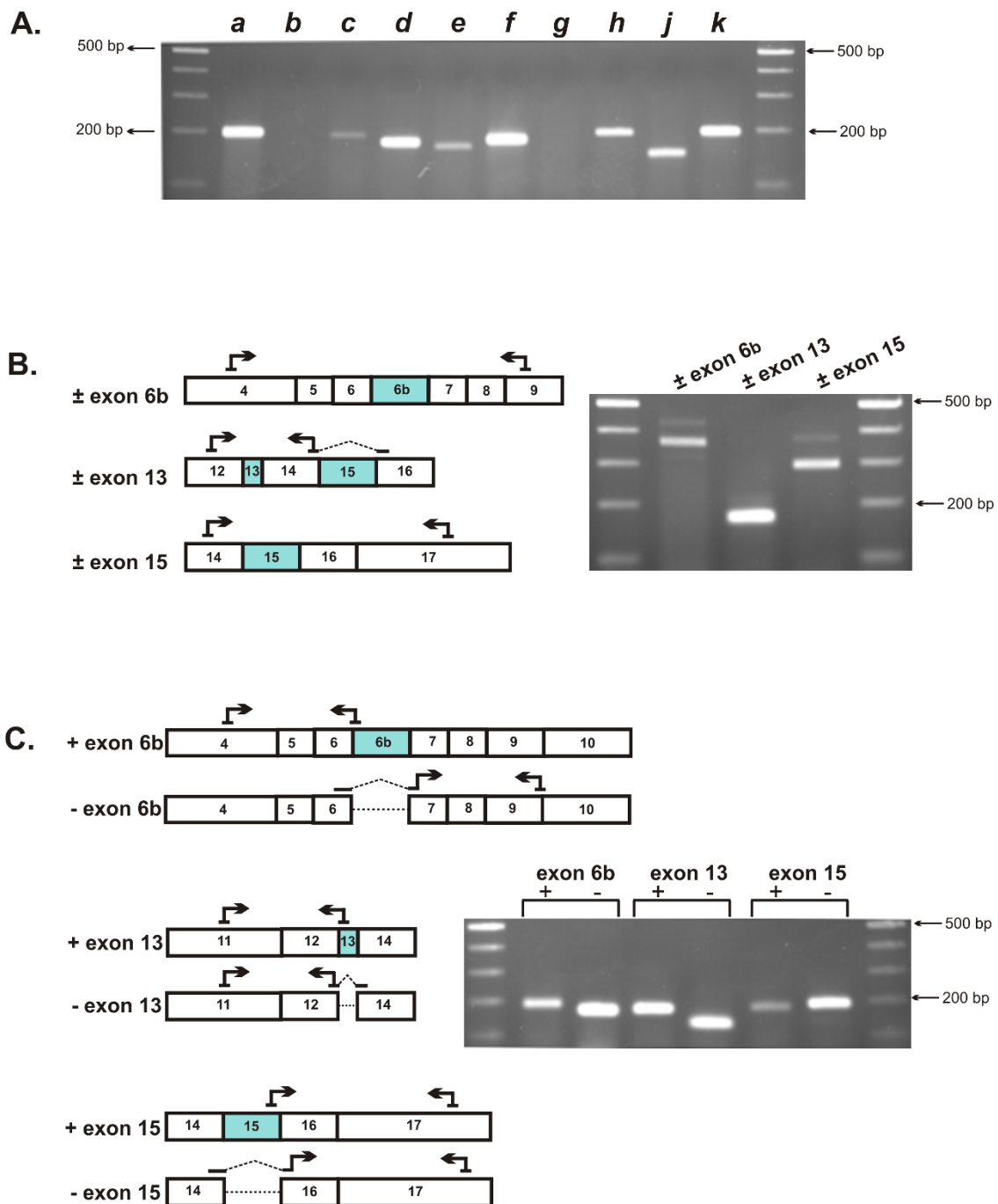


Figure 1 Identification of alternative *Tmem16a* exons 6b, 13 and 15 in mouse heart. **A.** Expression of *Tmem16* family members were analyzed in mouse heart using RT-PCR primers specific for each of the ten *Tmem16* paralogs. Amplification products were resolved on 2% agarose gels alongside a 100 bp marker. Fragments of the expected molecular size indicated the expression of *Tmem16a*, c, d, e, f, h, j and k paralogs in mouse heart. *Tmem16b* and g were not detected. **B.** Schematic representations of regions of *Tmem16a* RNA. Boxed numbers indicate exons relative to the *Tmem16a* gene. Alternative exon 6b (66 bp), exon 13 (12 bp) and exon 15 (78 bp) in the mouse *Tmem16a* coding sequence are highlighted. RT-PCR primers (\pm exon 6b, \pm exon 13, \pm exon 15), which amplify across each alternative exon are indicated. RT-PCR gel analysis of exon 6b, 13 and 15 *Tmem16a* variants expressed in mouse heart. Primers \pm exon 6b amplify a 367 and/or a 433 bp product, primers \pm exon 13 amplify a 165 and/or a 177 bp product, primers \pm exon 15 amplify a 297 and/or a 375 bp product. The upper bands correspond to *Tmem16a* variants that include the alternative exon and differ in size corresponding to the size of that exon. **C.** RT-PCR primer sets that span exon boundaries to selectively amplify individual alternative exons are indicated. Gel analysis of *Tmem16a* fragments expressed in mouse heart that either include or exclude exons 6b, 13 or 15. Each primer set yielded a single band of the expected size. RT-PCR products were sequenced for confirmation.

spans the junction of exons 14 and 16. Similarly, *Tmem16a* transcripts containing exon 15 (+exon 15) were specifically amplified using a primer internal to exon 15. RT-PCR gel analysis (Figure 1C) and fragment sequencing confirmed that *Tmem16a* variants are expressed in mouse heart that either exclude or include exon 6b, exon 13 and exon 15, identical to those we identified in mouse gastrointestinal tissues [24].

A comparison of the amino acid sequences of mouse and human alternative exons show a high similarity; the four amino acids (EAVK) of exon 13 are 100% identical, the 22 and 26 amino acids encoded by exon 6b and exon 15, share 95.5% and 80.8% identity, respectively. Considering the high percentage amino acid identity of these exon between the two species, we can expect that the regulatory properties attributed to these channel domains in human [22,23], will most likely confer similar functional roles in the mouse, in that, exon 6b may confer calcium sensitivity, exon 13 may contribute to voltage dependence and exon 15 may play a role in the activation and deactivation kinetics of this calcium activated chloride channel. The inclusion of alternative exons 6b, 13 and 15 would result in additional amino acids in intracellular channel domains and are not predicted to alter the eight transmembrane topology of the TMEM16A protein.

***Tmem16a* transcripts with combinations of alternative exons 6b, 13 and 15 create diversity**

A detailed investigation into the expression of various alternative exon combinations has not been reported for *Tmem16a*. To explore if different combinations of these alternative exons exist in mouse and human heart, we employed RT-PCR analysis to examine the region of the *Tmem16a* transcript encompassing alternative exons 6b, 13 and 15 (Figure 2). Eight *Tmem16a* variants may be generated due to alternative combinations of exon inclusion or exclusion (Figure 2A). RT-PCR analysis generated *Tmem16a* transcripts of various molecular sizes expressed in mouse and human heart (Figure 2B), corresponding to different combinations of *Tmem16a* alternative exon 6b, 13 or 15 inclusion or exclusion. The complexity of alternative exon combinations is difficult to resolve by size analysis alone, largely due to the micro exon 13 and two possible fragments of the same size (Figure 2A). Thus, the entire RT-PCR amplifications were cloned, and sequence analysis of multiple clones confirmed that at least six distinct *Tmem16a* splice variants consisting of various combinations of exons 6b, 13 and 15 are expressed in mouse and human heart.

Both mouse and human heart express the following three exon combinations: *Tmem16a* (-6b, +13, -15), *Tmem16a* (+6b, +13, -15), and *Tmem16a* (-6b, +13, +15). We did not identify *Tmem16a* transcripts consisting of

exon 6b alone (+6b, -13, -15) or a *Tmem16a* variant containing 6b and 15 but lacking exon 13 (+6b, -13, +15) in either mouse or human heart. It appears, at least in heart, that exon 6b is only expressed in the presence of exon 13. However, we did identify *Tmem16a* transcripts containing exon 15 in the absence of both exons 6b and 13 (-6b, -13, +15) in mouse heart. Interestingly, a *Tmem16a* transcript missing all three exons (-6b, -13, -15) was only identified in mouse heart, in agreement with the reported *Tmem16a* [GenBank: NM_178642] and although a human transcript variant 2 (-6b, -13, -15) [GenBank: NR_030691] exists we did not confirm its presence in human heart. All human *TMEM16A* transcripts contained exon 13, in agreement with [GenBank: NM_018043] (-6b, +13, +15). The largest *Tmem16a* variant consisting of all three exons was confirmed by sequence analysis in human heart. Although this *Tmem16a* variant was not confirmed in our screening of mouse heart clones, we cannot rule out its existence since our gel analysis indicates a band close to the expected size of this variant, albeit much weaker than in human (Figure 2B). Indeed, it is possible that different mouse and human tissues may express different combinations of these alternative exons, however, quantification of our data would not provide more information since the tissues examined in this study contain a mixed population of cells. The deduced amino acid sequence of mouse *TMEM16A* containing alternative exons combinations (6b, 13 and 15) all read in-frame, indicating that these alternative exons are additional channel components similar to those of human *TMEM16A* [22]. BLASTn searches of dbEST and Refseq RNA databases identified a number of mouse ESTs containing exon 6b and exon 13. Indeed, one mouse EST [GenBank: BI151426] was identified for the +6b, +13, -15 exon combination. EST supporting query sequences were identified for mouse [GenBank: BI685387] containing exon 13 alone (-6b, +13, -15). No ESTs were found in mouse containing both exon 13 and 15, however this is the exon combination in human that corresponds to *TMEM16A* [GenBank: NM_018043].

In addition to alternative exons 6b, 13 and 15, we also identified a number of novel *Tmem16a* splicing events in mouse and human heart; exon 10 and exon 14 exclusion, the inclusion of a novel exon, and two intron retention events.

Novel *Tmem16a* transcripts with exon 10 or exon 14 exclusion

We identified two previously unreported *Tmem16a* exon skipping events, exon 10 and exon 14, in mouse and human heart (Figure 3). Exclusion of exon 10 (135 bp) in *Tmem16a* RNA would result in an in-frame deletion of 45 amino acids in the channel protein. Exon 10 encodes a hydrophobic region predicted to be the first transmembrane spanning domain of *TMEM16A*.

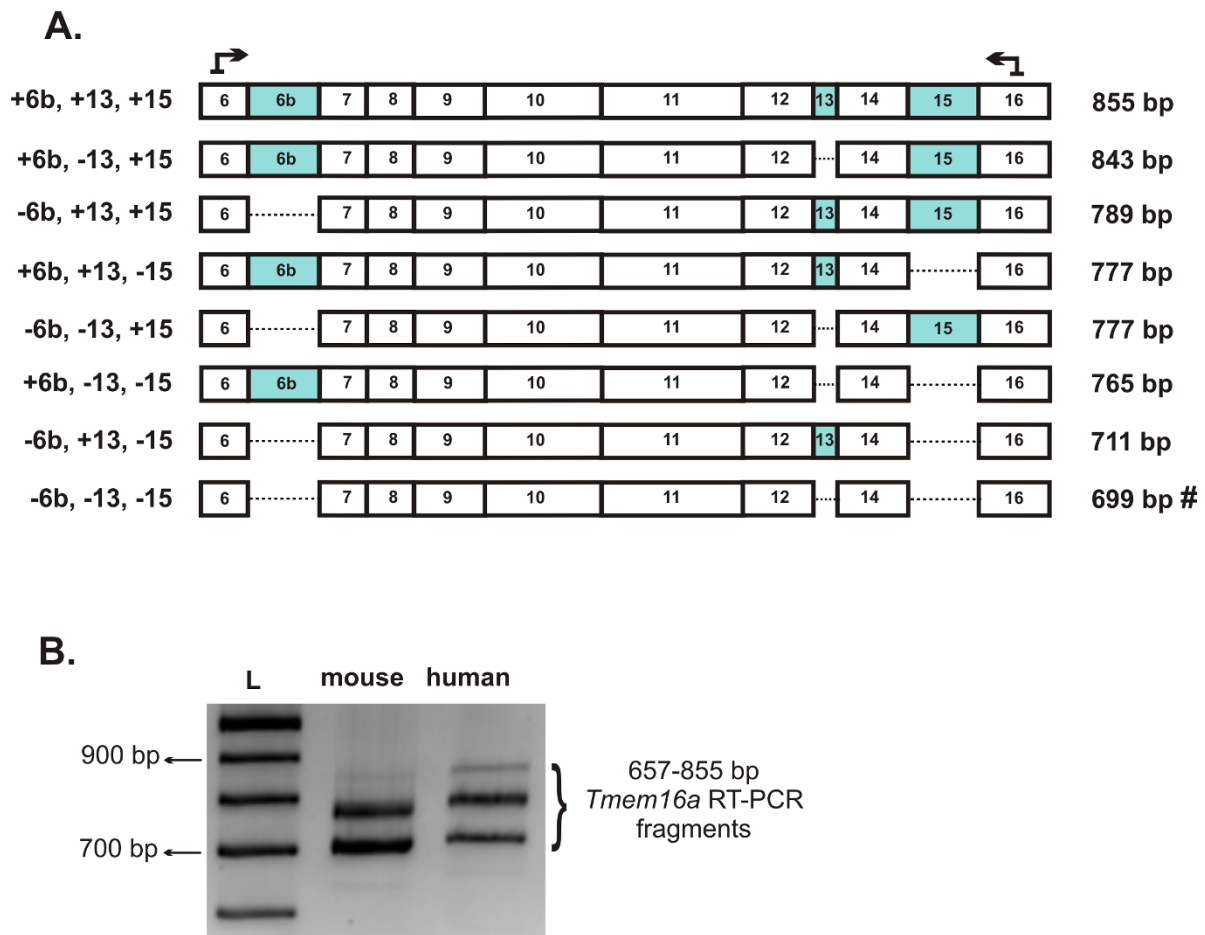


Figure 2 Multiple *Tmem16a* variants are expressed in heart due to different combinations of alternative exons 6b, 13 and 15. A. Cartoon indicating eight possible *Tmem16a* transcript variants as a result of combinations of exon 6b, 13 or 15 inclusion and/or exclusion. Dashed lines denote the exclusion of an alternative exon. Primers which span *Tmem16a* from exon 6 to exon 16, a region encompassing the three alternative exons (shaded), generate transcripts of various sizes depending upon which exons are amplified. The expected sizes of RT-PCR products are indicated. *Tmem16a* variant [GenBank: NM_178642] lacking all 3 exons is indicated (#). **B.** Gel analysis of *Tmem16a* RT-PCR fragments ranging between 657 and 855 bp were amplified. 100 bp ladder (L).

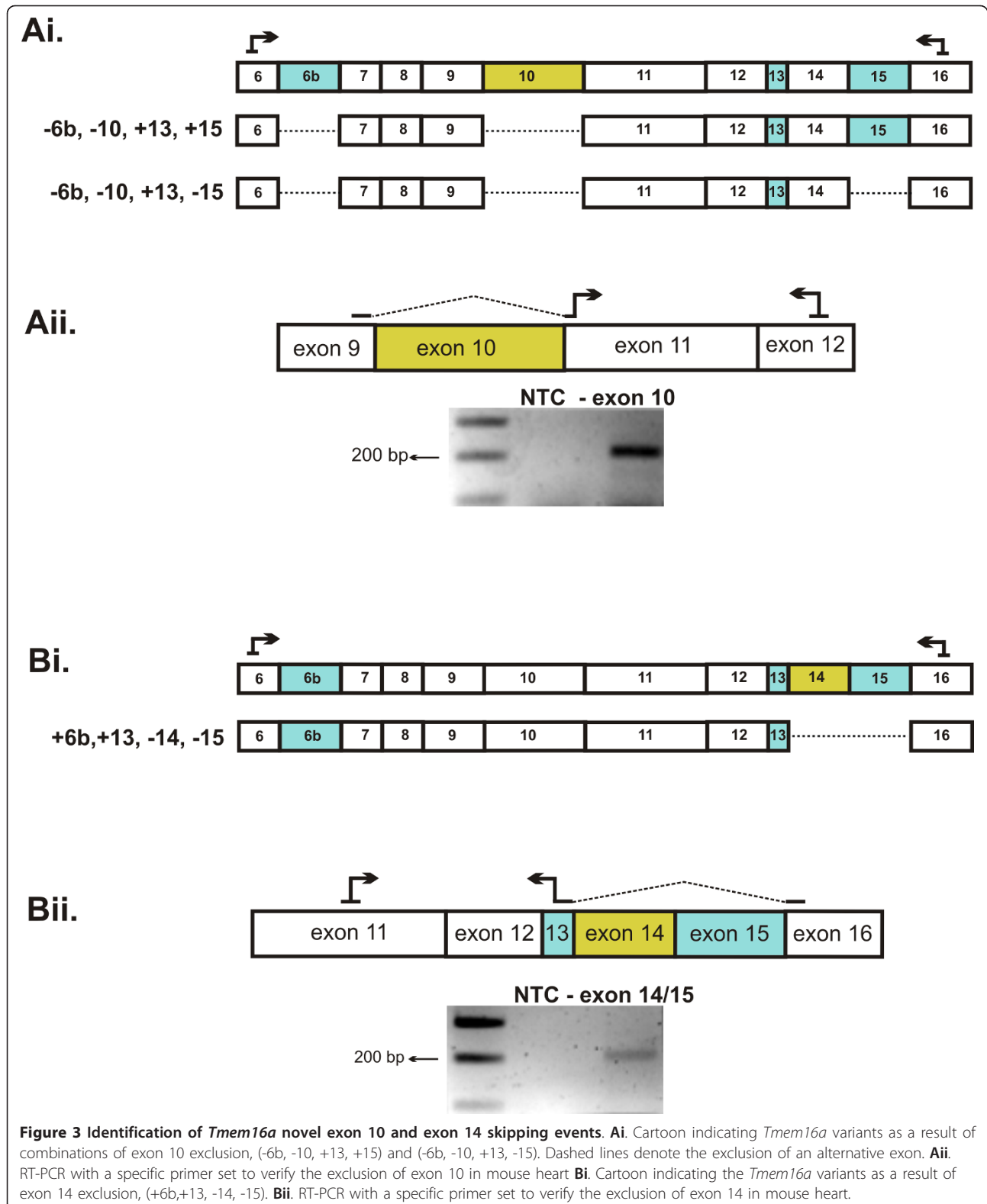
Therefore, exon 10 exclusion would result in a change in the transmembrane topology. We identified through sequencing two different *Tmem16a* (-10) transcripts, in that both transcripts lacked exon 6b and included exon 13, however, they differed in whether or not exon 15 was included. This is highlighted in the cartoon in Figure 3A. We employed an additional primer set to specifically amplify *Tmem16a* (-10) variants (Figure 3A) and sequence analysis confirmed the presence of these transcript variants in mouse and human heart.

Sequence analysis revealed that the *Tmem16a* (-14) variant included exons 6b and 13 and excluded exon 15 (Figure 3B). Exclusion of exon 14 (72 bp) in *Tmem16a* RNA would result in an in-frame deletion of 24 amino acids in the first intracellular loop of the TMEM16A channel. A PKC site is present in exon 14 at position S462 [GenBank: NP_848757] and one could speculate

that *Tmem16a* transcripts lacking exon 14 may encode channels that differ in modulation by PKC. Likewise, the expression of this variant was confirmed in mouse and human heart using primers which specifically amplify *Tmem16a* (-14) variants.

***Tmem16a* transcripts with a novel conserved exon 13b**

Sequence screening of our *Tmem16a* clone library, identified an unusual *Tmem16a* transcript that excluded alternative exons 6b, 13 and 15 yet contained an additional 120 nucleotides between exon 12 and exon 14. Evaluation of *Tmem16a* genomic sequence revealed that these 120 nucleotides are located within the 554 bp intronic region between exon 13 and 14 (Figure 4A) and are bordered by conserved 'GT-AG' acceptor and donor splice sites [27]. We assigned the additional sequence in this *Tmem16a* transcript as exon 13b. A close



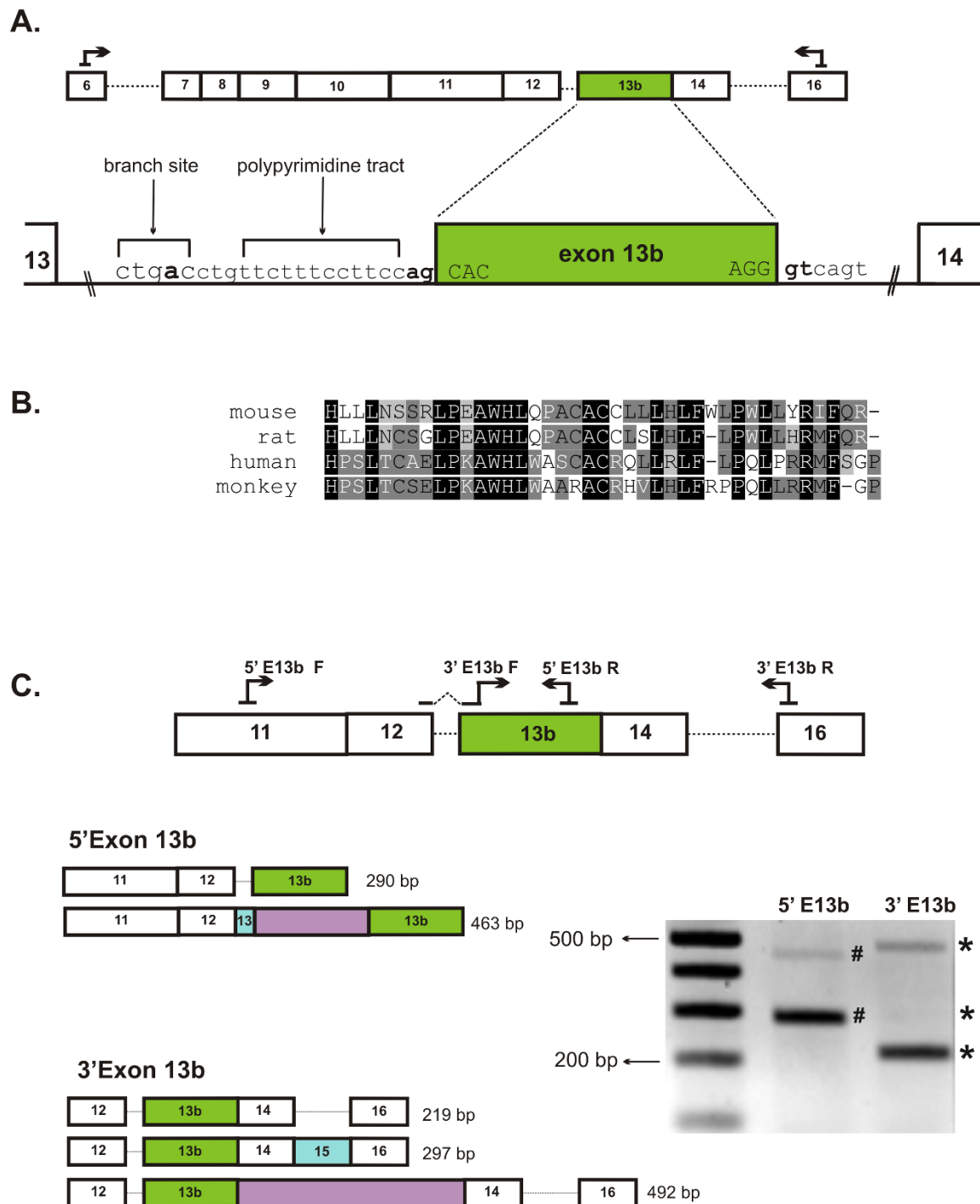


Figure 4 Identification of a novel exon 13b in *Tmem16a*. **A.** Cartoon representation of the novel exon 13b identified through sequence analysis of a *Tmem16a* fragment amplified using primers that span exons 6 through 16. Exon13b (120 bp) is highlighted. The genomic region between exon 13 and 14 is expanded to indicate the location of exon 13b, the splice and branch sites and the polypyrimidine tract. **B.** Alignment of the 40 amino acids encoded by exon 13b of mouse with the corresponding residues identified in rat, human and rhesus monkey. **C.** RT-PCR with primer sets 5'Exon13b and 3'Exon13b verified the expression of exon 13b in mouse heart. Cartoon of the amplification products generated with these primers is shown. Primer set 5'Exon13b produced two fragments, the 290 bp fragment consisted of exons 11, 12 and 13b; the 463 bp fragment consisted of exons 11, 12, 13 and 13b plus the entire intronic sequence between exon 13 and 13b. The 3'E13b primer set yielded three fragments. The 219 bp and 297 bp fragments included exons 12, 13b, 14, ± 15, 16, and the 492 bp fragment consisted of 12, 13b, 14, -15, 16 plus the intronic sequence between exon 13b and 14. The intron retention events are highlighted.

examination of the intronic sequence immediately upstream of exon 13b identified a conserved mammalian "CURAY" branchpoint sequence 18 nucleotides upstream of the 3' splice site (Figure 4A). The branchpoint (A nucleotide) is generally situated 18 to 40 nucleotides upstream of the 3' splice site and plays an important role in identifying this splice site [28,29]. An adjacent polypyrimidine tract, which increases the efficiency of branchpoint utilization [30], was also identified in this region (Figure 4A). Together, these findings add support that this 120 bp sequence is a true exon. Inclusion of exon 13b in the *Tmem16a* transcript would result in an in-frame addition of 40 amino acids in TMEM16A. This region is rich in hydrophobic leucine residues (12/40 residues being leucines). It is not surprising then that hydropathy analysis suggests that exon 13b inclusion may constitute an additional domain in the TMEM16A channel integral to the membrane.

Considering that the exon structures of *Tmem16a* are highly conserved amongst homologs, we investigated if similar novel exons could be identified in other species. A close examination of the genomic *Tmem16a* sequence from rat, human and rhesus monkey [GenBank: NC_005100, GenBank: NC_000011, GenBank: NC_007871,] revealed that similar sequences to mouse *Tmem16a* exon 13b, bordered by conserved splice sites could be identified. An alignment of the corresponding amino acid sequence of these four species (Figure 4B) demonstrates 97.6% overall consensus with an identity of 41.5%. Specific primers designed to amplify this novel exon in human heart were unable to identify its expression. Whether or not this exon is present in other human tissue types is unknown.

The expression of the novel exon 13b in mouse heart was investigated further using primer sets to specifically amplify the 5' and 3' regions surrounding the 120 bp exon (Figure 4C). Sequence analysis revealed some interesting observations. First, we confirmed that exon 13b is utilized in mouse heart. Secondly, exon 13b is present in several *Tmem16a* transcripts that differ in whether they also include or exclude alternative exons 13 or 15. Third, retention of the introns surrounding exon 13b increases the complexity of splicing in this region of *Tmem16a* transcript. RT-PCR with the primer set 5'Exon13b, in which primers bind within exon 11 and 13b produced two amplification products (Figure 4C). Sequencing analysis indicated one *Tmem16a* fragment consisted of exons 11, 12 and 13b and the other fragment consisted of exons 11, 12, 13, 13b plus the entire 161 bp intronic sequence between exon 13 and 13b (Figure 4C). The 3'Exon13b primer set, in which the primers hybridize across exon 12/13b junction and within exon 16, yielded three *Tmem16a* transcript fragments (Figure 4C). Two fragments differ in exon 15 inclusion/exclusion exons 12,

13b, 14, ± 15, 16, and an unexpected fragment consisting of exon 12, 13b, 14, -15, 16 plus the entire intronic sequence (273 bp) between exon 13b and 14 (Figure 4C). Intron retention events at the 5' and 3' of exon 13b are certainly the result of alternative *Tmem16a* splicing and not genomic contamination since the 5'Exon13b and 3'Exon13b primers span at least 14.4 kb and 4.4 kb of genomic sequence, respectively.

The intron retention events at the 5' and 3' of exon 13b would introduce a premature stop codon in the *Tmem16a* transcript, resulting in a truncated protein just after the "EAVK" amino acids encoded by exon 13. The complete retention of an intron in a mature transcript is one of the least expected forms of alternative splicing and may occur due to weak splice sites, cis-regulatory elements or short intron lengths [31]. Indeed, the introns between exons 13 and 13b and between exon 13b and 14 are two of the shortest in the *Tmem16a* genomic sequence (see Table 1). Intron retention can result in the insertion of a premature stop codon being introduced to the mature transcript which may then be degraded by nonsense mediated decay [32]. Indeed, decreasing the mRNA levels of certain genes can be the purpose of alternative splicing [32]. However, sometimes the retention of an intron in the coding region can have a biological effect. For example, an intron retaining isoform of the *KCNMA1* gene, which encodes the large conductance calcium-activated potassium channel (BK), facilitates splice variant regulation which contributes to structural and functional diversity of BK channel proteins in hippocampal neurons [33,34].

***Tmem16a* transcript scanning assay reveals additional novel splice variants**

It is clear from our analysis that *Tmem16a* transcript undergoes extensive splicing within the region between exons 6 and 16. In addition, not all of these exon inclusion/exclusion combinations are consistent between mouse and human. Indeed splicing events occurring at other regions of *Tmem16a* transcript may have important functional implications. Thus, we profiled the entire *Tmem16a* using overlapping RT-PCR primers to determine whether additional *Tmem16a* RNA splicing events occur in mouse and human heart. The transcript scanning assay and sequencing analysis revealed additional novel *Tmem16a* variants. These variants included exon 18 exclusion in both mouse and human *Tmem16a* and two alternative 3' donor sites, Δ3'exon 1 and Δ3'exon 21, in mouse. Details for mouse and human *Tmem16a* are summarized in Tables 2 and 3.

Exon 18 is 112 nucleotides and the exclusion of this exon shifts the encoded mouse TMEM16A out of frame at amino acid 1563 [GenBank: NP_848757], truncating the protein from 956 to 596 amino acids. Exon 18 encodes the fifth transmembrane spanning domain of TMEM16A [35]

Table 2 Mouse *Tmem16a* transcript scanning assay

Primer Set	Oligonucleotide sequences (5'→ 3')	<i>Tmem16a</i> region	Size (bp)	Alternative exon(s) identified
A	GAGGGAACCTCTGCGGACCGA (sense)	Exons 1-3	613	
	GCCAGGGCGCATGGATCTTC (antisense)		610	Δ3' Exon 1
B	GGCCTGGAGTTGGAGAATGACG (sense)	Exons 2-10	602	
	GTGTAGGCTCCAAGCCAGGCAA (antisense)		668	+ Exon 6b
C	GAACAACGTGCACCAAGGCCAAGTA (sense) TGGTGAAATAGGCTGGGAATCGGTC (antisense)	Exons 6-16	699	
			711	+ Exon 13
			777	+ Exon 15
			777	+ Exons 6b + 13
			789	+ Exons 13 + 15
			819	+ Exon 13b
			654	- Exons 10 +13 +15
			705	- Exons 6b +13 -14
D	TGGAGCACTGGAAACGGAAG (sense) ATACAGAGCTCCATGAGGCAGC (antisense)	Exons 12-20	625	
			637	+ Exon 13
E	ACCGACAAGGTGAAGCTGAC (sense) GACGCAACAAACAGGGTGAC (antisense)	Exons 16-22	731	
			619	- Exon 18
F	GAAGTTTACGGCTGCATTGC (sense) ATGTAGAGGTACACCAGGCGAG (antisense)	Exons 17-24	719	
			623	Δ3' Exon 21
G	GCCTCATGGAGCTCTGTATCC (sense) CACCCAGTCCACAAAGTCACTC (antisense)	Exons 20-26	767	
H	TGGTATAACATCCTCAGAGGTG (sense) TCACCTGGTGATGGTCAGAA (antisense)	Exons 23-26	656	

Table 3 Human *TMEM16A* transcript scanning assay

Primer Set	Oligonucleotide sequences (5'→ 3')	<i>Tmem16a</i> region	Size (bp)	Alternative exon(s) identified
A	ACAGGCCGCCACGATGAGGGTC (sense) GAGCCTGCATCCAGCGACGCC (antisense)	Exons 1-2	348	
B	AGGAGGGTGCGACACAGCGA (sense) ATTGGCCAGCAGGCTCGTGA (antisense)	Exons 2-7	582	+ Exon 6b
			648	
C	GAGAACGACGTGTACAAAGCCAAG (sense) TTAGTGAGGTAGGCTGGGAACCGAT (antisense)	Exons 6-16	714	+ Exon 13
			780	+ Exons 6b + 13
			792	+ Exons 13 + 15
			858	+ Exons 6b +13 +15
			579	- Exons 10 + 13
			657	- Exons 10 + 13+15
D	ACTGACAAAGTGAAGCTGACA (sense) TGTTCTGGATCAGCTGTTTC (antisense)	Exons 16-20	526	
			414	- Exon 18
E	TTTCCGTTCTCCGAATGG (sense) CTTCCAATGCCTCTGAGGATA (antisense)	Exons 19-23	460	
F	TGCTACTGAGCTCCGAAGGCCG (sense) ACGATGACAAACGCCAGCCGG (antisense)	Exons 22-25	384	
G	AGTAAGAACGGGACCATGCACGG (sense) CGCTGGCATAGCTACAGGACGC (antisense)	Exons 24-26	509	

and exclusion of exon 18 would result in a C-terminus truncated TMEM16A protein containing four membrane spanning domains (Figure 5A). Translation of mouse TMEM16A yields a protein of ~110kDa. The exclusion of exon 18 in the mouse transcript could result in a truncated TMEM16A protein of ~60 -75 kDa (depending upon which other alternative exons reported in this study are also included or excluded). Interestingly, two independent studies have reported an additional signal on Western blots for TMEM16A [25,36] which were much lower (~80 kDa) than the expected 110 kDa. From the results presented in this study, it is possible that the lower molecular weight band corresponds to an alternatively spliced transcript that encodes a truncated TMEM16A protein.

The $\Delta 3'$ exon 1 and $\Delta 3'$ exon 21 alternative donor sites are the result of wobble splicing occurring at donor splice sites located in close proximity, commonly known as tandem splice sites. Alternative splicing at tandem splice sites occurs frequently in many species and can result in subtle variations in transcripts and the proteins that they encode [37]. Use of the *Tmem16a* $\Delta 3'$ exon 1 splice site, results in the exclusion of the last 3 nucleotides (GTG) of

exon 1. The mouse *Tmem16a* genomic sequence was queried against the TassDB database of alternative tandem splice sites [38], and the $\Delta 3'$ exon 1 was recognized as tandem splicing at donor splice site with the motif GYNGYN. Indeed, a BLASTn search of the EST database revealed 27 ESTs without this 3' GTG and two ESTs that contained it. This alternative splice event is not expected to alter TMEM16A protein since exon 1 is non-coding. Skipping of exon 1 and part of exon 2 has been reported in human TMEM16A [13], however, Ferrera et al failed to identify transcripts lacking this region [22] and considered that its splicing may be under the control of an alternative promoter and influenced by certain physiological or pathophysiological conditions. Indeed, a recent study showed that a novel TMEM16A variant with an alternative 5' end is highly expressed in gastric smooth muscle of patients with diabetic gastroparesis compared with controls [23]. Apart from $\Delta 3'$ exon 1 tandem splice site, our study did not identify additional variation at the 5' end. The $\Delta 3'$ exon 21 tandem splice site would result in 4 additional (GTGA) nucleotides at the 3' end of exon 21. This is predicted to shift the protein out of frame at amino acid M702 [GenBank: NP_848757], resulting in a truncated TMEM16A protein with an altered C-terminus of ~84 kDa. According to TassDB2 [39] this tandem splice site is conserved in human, dog and chicken *Tmem16a* sequence.

Distribution of novel *Tmem16a* alternative splice variants in other tissues

This study focused on identifying *Tmem16a* splice variants in heart. We extended this analysis to investigate if these novel variants are expressed in other mouse tissues from which a calcium-activated chloride current can be recorded. Initially, we confirmed *Tmem16a* expression in mouse brain, lung, stomach (antrum), small intestine, colon, kidney and bladder tissues (data not shown). All organs were dissected out with their attached vasculature. Total RNA obtained from each of these organs therefore contains a mixed population of cells. We then examined the expression of the following exons: +6b, -10, +13, +13b, -14, +15 and -18. The distribution of *Tmem16a* alternative exon variants in these mouse tissues is summarized (Table 4). In addition to heart, all of the tissues examined express the following variants; +6b, -10, +13, +13b and +15. The -14 exon variant was only detected in heart, lung, small intestine and colon. The -18 exon variant was detected in all tissues examined apart from kidney. The molecular diversity of *Tmem16a* may contribute to numerous proteomic variations of TMEM16A channels that may fine-tune channel functions in specific tissue types.

Conclusion

This report provides details of *Tmem16a* genomic organization and our analyses have detected previously

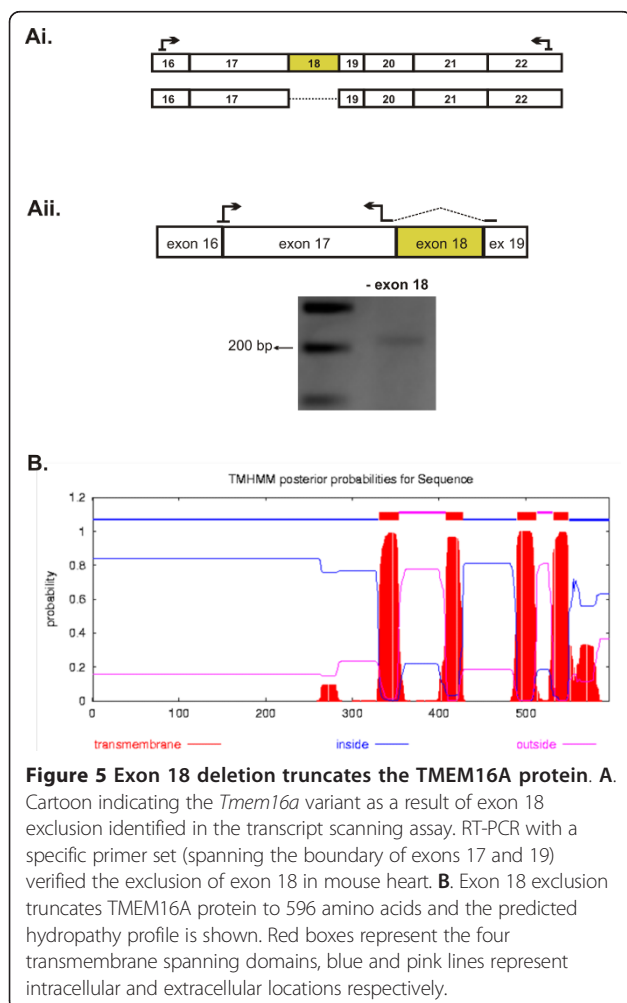


Table 4 Distribution of *Tmem16a* exon variants in mouse tissues

	heart	brain	lung	stomach	s.int.	colon	kidney	bladder
+ exon 6b	++	+++	+++	+++	+++	+++	+++	+
- exon 10	+	+	+	+	+	+	+	+
+ exon 13	+++	+++	+++	+++	+++	+++	+++	++
+ exon 13b	++	+++	+++	++	+++	+++	++	+
- exon 14	+	n.d.	+	n.d.	+	+	n.d.	n.d.
+ exon 15	++	++	+	+++	+++	+++	+++	+
- exon 18	+	+	+	+	+++	+++	n.d.	+

s.int. (small intestine) +++ indicates high, ++ moderate and + low expression. n.d., not detected.

unidentified alternative exons. We identified *Tmem16a* transcript variants consisting of different exon usage events involving exons 6b, 10, 13, 14, 15 and 18. Many of these exons are expressed in various combinations. A number of other splicing events including a novel exon 13b, tandem splice sites of exon 1 and 21 and two intron retention events were also identified. The alternative splicing events identified here indicate that a varied population of TMEM16A channels is expressed in mouse heart and other tissues. The heart is a highly heterogeneous tissue composed of numerous cell types tailored for specialized function. It is possible that many *Tmem16a* variants can be co-expressed in the same cells, or differentially distributed in distinct cell types within the myocardium. Determining the localization of different *Tmem16a* isoforms within tissues has important implications with regard to the function of *Tmem16a*. The functional consequence of TMEM16A channel diversity remains to be determined. We can speculate however, that TMEM16A variants would create channels with altered biophysical properties, such as that reported for exon 6b, 13 and 15 in TMEM16A [22,23]. It is also possible that regulation of the channels may be altered since several of these alternatively spliced exons contain phosphorylation sites and interacting domains, for example, PKC and CamKII (exon 18), PKA (exon 6b), Erk-D domain (exon 10) and a Src-SH3 domain (exon 15). TMEM16A channels have been shown to form homodimers [40,41], therefore, it is likely that TMEM16A variants may interact with each other to form functional channels in a similar manner to that reported for the hERG family [42]. Another possibility is that alternatively spliced isoforms may associate with additional accessory proteins. It is evident from this study that alternative splicing is an exquisite mechanism that operates to diversify TMEM16A channel structures by the combinatorial selection of alternatively spliced events. Future recombinant expression of different *Tmem16a* variants will reveal their physiological role.

Additional material

Additional file 1: Tables S1 and S2. TABLE S1: Primers used for RT-PCR of *Tmem16* paralogs. This table lists the GenBank accession number for *Gapdh* and *Tmem16* paralogs, the oligonucleotide sequence of each primer and the expected amplicon sizes. **TABLE S2: Primers used for RT-PCR of *Tmem16a* exon variants.** This table lists the primer name, the oligonucleotide sequence of each primer, the annealing temperature of each primer set and the expected amplicon sizes.

Acknowledgements and Funding

The authors would also like to acknowledge Carly Gertler for excellent technical assistance. This project was supported by a NIH grant 1R01HL091238 to FCB.

Authors' contributions

FCB and KEOD conceived the design of the study and prepared the manuscript. KEOD and RAP isolated RNA, constructed the libraries and prepared samples for sequencing. KEOD analyzed the sequencing data. All authors have read and approved the final manuscript.

Received: 23 March 2011 Accepted: 8 August 2011

Published: 8 August 2011

References

- Black DL: Mechanisms of alternative pre-messenger RNA splicing. *Annu Rev Biochem* 2003, **72**:291-336.
- Britton FC, Wang GL, Huang ZM, Ye L, Horowitz B, Hume JR, Duan D: Functional characterization of novel alternatively spliced CIC-2 chloride channel variants in the heart. *J Biol Chem* 2005, **280**:25871-25880.
- Cunha SR, Le SS, Schott JJ, Mohler PJ: Exon organization and novel alternative splicing of the human ANK2 gene: implications for cardiac function and human cardiac disease. *J Mol Cell Cardiol* 2008, **45**(6):724-734.
- Dally S, Corvazier E, Bredoux R, Bobe R, Enouf J: Multiple and diverse coexpression, location, and regulation of additional SERCA2 and SERCA3 isoforms in nonfailing and failing human heart. *J Mol Cell Cardiol* 2010, **48**(4):633-644.
- George CH, Rogers SA, Bertrand BM, Tunwell RE, Thomas NL, Steele DS, Cox EV, Pepper C, Hazeel CJ, Claycomb WC, Lai FA: Alternative splicing of ryanodine receptors modulates cardiomyocyte Ca²⁺ signaling and susceptibility to apoptosis. *Circ Res* 2007, **100**(6):874-883.
- Kupershmidt S, Snyders DJ, Raes A, Roden DM: A K⁺ channel splice variant common in human heart lacks a C-terminal domain required for expression of rapidly activating delayed rectifier current. *J Biol Chem* 1998, **273**(42):27231-27235.
- Liao P, Yong TF, Liang MC, Yue DT, Soong TW: Splicing for alternative structures of Cav1.2 Ca²⁺ channels in cardiac and smooth muscles. *Cardiovasc Res* 2005, **68**(2):197-203.
- Schroeter A, Walzik S, Blechschmidt S, Haufe V, Benndorf K, Zimmer T: Structure and function of splice variants of the cardiac voltage-gated sodium channel Na(v)1.5. *J Mol Cell Cardiol* 2010, **49**(1):16-24.

9. Xu Y, Dong PH, Zhang Z, Ahmmed GU, Chiamvimonvat N: **Presence of a calcium-activated chloride current in mouse ventricular myocytes.** *Am J Physiol Heart Circ Physiol* 2002, **283**:H302-H314.
10. Hiraoka M, Kawano S, Hirano Y, Furukawa T: **Role of cardiac chloride currents in changes in action potential characteristics and arrhythmias.** *Cardiovasc Res* 1998, **40**:23-33.
11. Hume JR, Duan D, Collier ML, Yamazaki J, Horowitz B: **Anion transport in heart.** *Physiol Rev* 2000, **80**:31-81.
12. Sorota S: **Insights into the structure, distribution and function of the cardiac chloride channels.** *Cardiovasc Res* 1999, **42**:361-376.
13. Caputo A, Caci E, Ferrera L, Pedemonte N, Barsanti C, Sondo E, Pfeffer U, Ravazzolo R, Zegarra-Moran O, Galletta LJ: **TMEM16A, a membrane protein associated with calcium-dependent chloride channel activity.** *Science* 2008, **322**(5901):590-594.
14. Schroeder BC, Cheng T, Jan YN, Jan LY: **Expression cloning of TMEM16A as a calcium-activated chloride channel subunit.** *Cell* 2008, **134**:1019-1029.
15. Yang YD, Cho H, Koo JY, Tak MH, Cho Y, Shim WS, Park SP, Lee J, Lee B, Kim BM, Raouf R, Shin YK, Oh U: **TMEM16A confers receptor-activated calcium-dependent chloride conductance.** *Nature* 2008, **455**(7217):1210-1215.
16. Pifferi S, Dibattista M, Menini A: **TMEM16B induces chloride currents activated by calcium in mammalian cells.** *Pflugers Arch* 2009, **458**(6):1023-1038.
17. Schreiber R, Uliyakina I, Kongsuphol P, Warth R, Mirza M, Martins JR, Kunzelmann K: **Expression and function of epithelial anoctamins.** *J Biol Chem* 2010, **285**(10):7838-7845.
18. Stohr H, Heisig JB, Benz PM, Schoberl S, Milenkovic VM, Strauss O, Aartsen WM, Wijnholds J, Weber BH, Schulz HL: **TMEM16B, a novel protein with calcium-dependent chloride channel activity, associates with a presynaptic protein complex in photoreceptor terminals.** *J Neurosci* 2009, **29**:6809-6818.
19. Hartzell C, Putzier I, Arreola J: **Calcium-activated chloride channels.** *Annu Rev Physiol* 2005, **67**:719-758.
20. Huang X, Godfrey TE, Gooding WE, McCarty KS Jr, Gollin SM: **Comprehensive genome and transcriptome analysis of the 11q13 amplicon in human oral cancer and synteny to the 7F5 amplicon in murine oral carcinoma.** *Genes Chromosomes Cancer* 2006, **45**:1058-1069.
21. O'Driscoll KE, Hatton WJ, Britton FC: **Alternative splicing of the murine Tmem16a transcript in heart.** *FASEB J* 2010, **24**:28.
22. Ferrera L, Caputo A, Ubbly I, Bussani E, Zegarra-Moran O, Ravazzolo R, Pagani F, Galletta LJ: **Regulation of TMEM16A chloride channel properties by alternative splicing.** *J Biol Chem* 2009, **284**(48):33360-33368.
23. Mazzone A, Bernard CE, Strege PR, Beyder A, Galletta LJ, Pasricha PJ, Rae JL, Parkman HP, Linden DR, Szurszewski JH, Ordog T, Gibbons SJ, Farrugia G: **Altered expression of Ano1 variants in human diabetic gastroparesis.** *J Biol Chem* 2011, **286**(15):13393-13403.
24. Hwang SJ, Blair PJ, Britton FC, O'Driscoll KE, Hennig G, Bayguinov YR, Rock JR, Harfe BD, Sanders KM, Ward SM: **Expression of anoctamin 1/TMEM16A by interstitial cells of Cajal is fundamental for slow wave activity in gastrointestinal muscles.** *J Physiol* 2009, **587**:4887-4904.
25. Davis AJ, Forrest AS, Jepps TA, Valencik ML, Wiwchar M, Singer CA, Sones WR, Greenwood IA, Leblanc N: **Expression profile and protein translation of TMEM16A in murine smooth muscle.** *Am J Physiol Cell Physiol* 2010, **299**(5):C948-C959.
26. Kozak M: **Interpreting cDNA sequences: some insights from studies on translation.** *Mamm Genome* 1996, **7**:563-574.
27. Smith CW, Valcarcel J: **Alternative pre-mRNA splicing: the logic of combinatorial control.** *Trends Biochem Sci* 2000, **25**(8):381-388.
28. Reed R, Maniatis T: **Intron sequences involved in lariat formation during pre-mRNA splicing.** *Cell* 1985, **41**(1):95-105.
29. Rautmann G, Breathnach R: **A role for branchpoints in splicing in vivo.** *Nature* 1985, **315**(6018):430-432.
30. Coolidge CJ, Seely RJ, Patton JG: **Functional analysis of the polypyrimidine tract in pre-mRNA splicing.** *Nucleic Acids Res* 1997, **25**(4):888-896.
31. Sakabe NJ, de Souza SJ: **Sequence features responsible for intron retention in human.** *BMC Genomics* 2007, **8**:59.
32. Lareau LF, Green RE, Bhatnagar RS, Brenner SE: **The evolving roles of alternative splicing.** *Curr Opin Struct Biol* 2004, **14**(3):273-282.
33. Bell TJ, Miyashiro KY, Sul JY, McCullough R, Buckley PT, Jochems J, Meaney DF, Haydon P, Cantor C, Parsons TD, Eberwine J: **Cytoplasmic BK (Ca) channel intron-containing mRNAs contribute to the intrinsic excitability of hippocampal neurons.** *Proc Natl Acad Sci USA* 2008, **105**(6):1901-1906.
34. Bell TJ, Miyashiro KY, Sul JY, Buckley PT, Lee MT, McCullough R, Jochems J, Kim J, Cantor CR, Parsons TD, Eberwine JH: **Intron retention facilitates splice variant diversity in calcium-activated big potassium channel populations.** *Proc Natl Acad Sci USA* 2010, **107**(49):21152-21157.
35. Hartzell HC, Yu K, Xiao Q, Chien LT, Qu Z: **Anoctamin/TMEM16 family members are Ca²⁺-activated Cl⁻ channels.** *J Physiol* 2009, **587**:2127-2139.
36. He Q, Halm ST, Zhang J, Halm DR: **Activation of the basolateral membrane Cl⁻ conductance essential for electrogenic K⁺ secretion suppresses electrogenic Cl⁻ secretion.** *Exp Physiol* 2011, **96**(3):305-316.
37. Hiller M, Platzer M: **Widespread and subtle: alternative splicing at short-distance tandem sites.** *Trends Genet* 2008, **24**(5):246-255.
38. Hiller M, Nikolajewa S, Huse K, Szafrański K, Rosenstiel P, Schuster S, Backofen R, Platzer M: **TassDB: a database of alternative tandem splice sites.** *Nucleic Acids Res* 2007, **35** Database: D188-D192.
39. Sinha R, Lenser T, Jahn N, Gausmann U, Friedel S, Szafrański K, Huse K, Rosenstiel P, Hampe J, Schuster S, Hiller M, Backofen R, Platzer M: **TassDB2 - A comprehensive database of subtle alternative splicing events.** *BMC Bioinformatics* 2010, **11**:216.
40. Fallah G, Romer T, Detro-Dassen S, Braam U, Markwardt F, Schmalzing G: **TMEM16A(a)/anoctamin-1 shares a homodimeric architecture with CLC chloride channels.** *Mol Cell Proteomics* 2011, **10**(2):M110.
41. Sheridan JT, Worthington EN, Yu K, Gabriel SE, Hartzell HC, Tarran R: **Characterization of the Oligomeric Structure of the Ca²⁺-activated Cl⁻ Channel Ano1/TMEM16A.** *J Biol Chem* 2011, **286**(2):1381-1388.
42. Guasti L, Crociani O, Redaelli E, Pillozzi S, Polvani S, Masselli M, Mello T, Galli A, Amedei A, Wymore RS, Wanke E, Arcangeli A: **Identification of a posttranslational mechanism for the regulation of hERG1 K⁺ channel expression and hERG1 current density in tumor cells.** *Mol Cell Biol* 2008, **28**(16):5043-5060.

doi:10.1186/1471-2199-12-35

Cite this article as: O'Driscoll et al.: Increased complexity of *Tmem16a*/Anoctamin 1 transcript alternative splicing. *BMC Molecular Biology* 2011 12:35.

Submit your next manuscript to BioMed Central and take full advantage of:

- Convenient online submission
- Thorough peer review
- No space constraints or color figure charges
- Immediate publication on acceptance
- Inclusion in PubMed, CAS, Scopus and Google Scholar
- Research which is freely available for redistribution

Submit your manuscript at
www.biomedcentral.com/submit

